Multi-channel optical instrument for near-infrared imaging of tissue

Maria Angela Franceschini, Sergio Fantini, Scott A. Walker,
John S. Maier, William W. Mantulin, and Enrico Gratton

Laboratory for Fluorescence Dynamics
University of Illinois at Urbana-Champaign
Urbana, IL, 61801-3080

ABSTRACT

Our research is aimed at the development of a frequency-domain instrument for conducting non-invasive, real-time, near-infrared optical tomography of tissue *in vivo*. Our goal is to reconstruct a spatial map of the optical properties of a strongly scattering medium in a semi-infinite-geometry sampling configuration. Specifically, we focus our attention on the absorption coefficient (μ_a) and the reduced scattering coefficient (μ_s') of the medium. We have developed a frequency-domain measurement protocol (which we call pre-calibrated), which permits one to recover the values of μ_a and μ_s' of a uniform tissue-like phantom from a measurement at a single source-detector separation and a single modulation frequency. It requires a preliminary reference measurement on a calibration sample of known optical properties before the measurement on the investigated sample. This approach is in principle rigorous only in macroscopically homogenous media. We have verified that the equations valid for uniform media can still be applied to yield qualitative information on the optical nature of the inhomogeneity if the effect of macroscopic inhomogeneities on the measured phase and intensity is not too large. *In vitro* measurements on turbid media containing scattering and absorbing inhomogeneities, with optical properties very similar to the background medium, gave encouraging results. We plan to implement this measurement protocol in a multi-source, multi-detector instrument for optical tomography.

Keywords: Frequency-domain, optical imaging, biological tissue, turbid medium, absorption coefficient, reduced scattering coefficient.

1. INTRODUCTION

We are working on the development of a frequency domain optical instrument for non-invasive tissue imaging in the near infrared. Our objective is to be able to reconstruct, at least qualitatively, the spatial map of the optical properties of the examined tissue. To this end, we plan to apply a weighted back-projection method[1] which requires readings from a number of source-detector pairs. In principle these different source-detector geometrical configurations can be obtained by mechanically scanning either the source, or the detector, or both. The disadvantage of such a procedure is the time limitation introduced by the mechanical scan. To avoid this limitation, we propose to electronically multiplex a number of light sources and collect data with a number of optical detectors. By appropriately positioning light

 0-8194-1736-X/95/$6.00

sources and optical detectors, we can have a large number of source-detector geometrical configurations. The total acquisition time will be as short as a few seconds. The basic requirement for this approach is to assign a reading of the optical properties of the medium to each source-detector pair. This determination of the optical parameters μ_a and μ_s' from data at a single source-detector distance, and a single modulation frequency is the subject of this paper. We present the development of the single-distance, single-frequency (or pre-calibrated) measurement protocol to determine μ_a and μ_s'. On the basis of *in vitro* measurements under controlled conditions, we examine the performance of this method in qualitatively evaluating the optical properties of macroscopic inhomogeneities embedded in the turbid medium. Finally, we indicate some limitations to this approach, which should be considered in instrument design.

2. DETERMINATION OF ABSORPTION AND REDUCED SCATTERING COEFFICIENTS IN IMAGING APPLICATIONS

In a macroscopically homogeneous, strongly scattering, infinite medium, the expressions for the frequency-domain quantities ψ_{DC} (the average photon flux), ψ_{AC} (the amplitude of the photon flux oscillations), and Φ (the phase of the photon flux) derived from the diffusion equation are the following:[2]

$$\psi_{DC} = \frac{S}{(4\pi)^2 D} \frac{\exp\left(-r\sqrt{\frac{\mu_a}{D}}\right)}{r} \tag{1a}$$

$$\psi_{AC} = \frac{SA}{(4\pi)^2 D} \frac{\exp\left(-r\sqrt{\frac{\mu_a}{2D}}\left(\sqrt{1+\left(\frac{\omega}{\nu\mu_a}\right)^2}+1\right)^{1/2}\right)}{r} \tag{1b}$$

$$\Phi = r\sqrt{\frac{\mu_a}{2D}}\left(\sqrt{1+\left(\frac{\omega}{\nu\mu_a}\right)^2}-1\right)^{1/2} + \Phi_s \tag{1c}$$

where r is the distance between source and detector (r must be much greater than the photon mean free path), v is the velocity of light in the medium (given by c/n where c is the velocity of light in vacuum and n is the index of refraction of the medium), ψ is the photon flux (in units of photons$\times$cm$^{-2}\times$sec^{-1}), D is the diffusion coefficient defined as $1/(3\mu_a + 3\mu_s')$, S is the source strength (in photons per second), A is the modulation of the source (the modulation of an intensity modulated light source is defined as the ratio of the AC to the DC component of the intensity), and Φ_s is the phase source term. The unknowns in the expressions for the measured quantities are the source terms S, A and Φ_s, and the optical parameters of the medium (μ_a, μ_s' and the index of refraction n). Since μ_a and n are not separable, the index of refraction of the medium is usually considered to be known. Moreover, the measured intensities depend on the detector response function, and on the optical coupling with the medium. The source terms, the detector response function and the optical coupling can be either determined or eliminated by performing an additional reference measurement, provided that they remain the same in the two measurements.

The two common ways to perform this referenced measurement consist of acquiring data either at two different source-detector distances, or at two different modulation frequencies. In the case of a macroscopically homogeneous infinite medium and for modulation frequencies less than 300 MHz, we have analytically and experimentally shown that a multi-distance measurement is more accurate and more precise than a multi-frequency measurement.[3,4] For this reason, our studies in spectroscopy have employed the multi-distance approach. The measured quantities $\ln(r\psi_{DC})$, $\ln(r\psi_{AC})$ and Φ show a linear dependence on r. The slopes of these straight lines are function of μ_a and μ_s' (and of the known parameters ω and v). The unknown source terms S, A and Φ_s appear only in the intercept factors. Consequently, a measurement of the slopes, performed by collecting data at different source-detector distances, can determine the optical coefficients without requiring the knowledge of the source terms. Moreover μ_a and μ_s' can be obtained from explicit analytical functions of the slopes. This fact reduces the computation time and permits one to accomplish real-time monitoring.

The multi-distance measurement protocol discussed above is accurate and precise in tissue spectroscopy. However, it presents a drawback in imaging applications. Since the probed three dimensional spatial region is different at various source-detector separations, the effect of an optical inhomogeneity on the measured quantities changes for different source-detector pairs. This concept is shown in Fig. 1, where the effect of an inhomogeneity is pictorially associated with the photon path distributions.

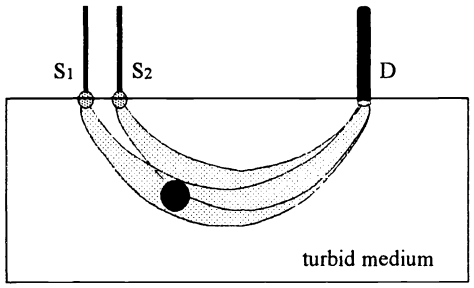

Fig. 1. The spatial region actually sampled by source-detector couple S_1-D is different than that sampled by S_2-D. In the case depicted in the figure, where the optical inhomogeneity affects data collected from S_1 to a greater extent than data detected from S_2, the multi-distance protocol is not appropriate.

The photon path distributions are strongly affected by changes in distance between source and detector. Different modulation frequencies also change the shape of the light bundle, even if this effect is smaller than that associated to variations in r.

In this paper, we propose a different experimental protocol that permits one to recover μ_a and μ_s' relative to a localized spatial region: we call it the pre-calibrated approach. This measurement protocol consists of a preliminary reference measurement on a calibration sample of known optical properties μ_{a0} and μ_{s0}'. By assuming that source terms, detector response function, and optical coupling with the medium do not vary by changing sample, a measurement on the investigated sample yields the values of μ_a and μ_s'. By using this protocol, the values of μ_a and μ_s' are obtained from a single source-detector pair and single modulation frequency, and hence are relative to a well defined spatial region.

In the infinite geometry boundary conditions, from Eqs. (1*a*), (1*b*) and (1*c*) we derive the following equations:

$$\frac{D\psi_{DC}}{D_0\psi_{DC0}} = \exp\left(r\sqrt{\frac{\mu_{a0}}{D_0}} - r\sqrt{\frac{\mu_a}{D}}\right) \tag{2a}$$

$$\frac{D\psi_{AC}}{D_0\psi_{AC0}} = \exp\left(r\left[\sqrt{\frac{\mu_{a0}}{2D_0}}\left(\sqrt{1+\left(\frac{\omega}{v\mu_{a0}}\right)^2}+1\right)^{1/2} - \sqrt{\frac{\mu_a}{2D}}\left(\sqrt{1+\left(\frac{\omega}{v\mu_a}\right)^2}+1\right)^{1/2}\right]\right) \tag{2b}$$

$$\Phi - \Phi_0 = -r\left[\sqrt{\frac{\mu_{a0}}{2D_0}}\left(\sqrt{1+\left(\frac{\omega}{v\mu_{a0}}\right)^2}-1\right)^{1/2} - \sqrt{\frac{\mu_a}{2D}}\left(\sqrt{1+\left(\frac{\omega}{v\mu_a}\right)^2}-1\right)^{1/2}\right] \tag{2c}$$

where the quantities with subscript 0 (μ_{a0}, μ_{s0}', D_0, ψ_{DC0}, Φ_0) are relative to the calibration measurement. After some algebra we find the following equations:

using DC and phase:
$$\ln\frac{D}{D_0} = \alpha_{DC} - \sqrt{\left(\frac{r^2\omega}{2v\gamma D}\right)^2 - \gamma^2} \tag{3a}$$

using AC and phase:
$$\ln\frac{D}{D_0} = \alpha_{AC} - \frac{r^2\omega}{2v\gamma D} \tag{3b}$$

where:
$$\alpha_{DC} = \ln\left(\frac{\psi_{DC0}}{\psi_{DC}}\right) + r\sqrt{\frac{\mu_{a0}}{D_0}},$$

$$\alpha_{AC} = \ln\left(\frac{\psi_{AC0}}{\psi_{AC}}\right) + r\sqrt{\frac{\mu_{a0}}{2D_0}}\left(\sqrt{1+\left(\frac{\omega}{v\mu_{a0}}\right)^2}+1\right)^{1/2},$$

$$\gamma = \Phi - \Phi_0 + r\sqrt{\frac{\mu_{a0}}{2D_0}}\left(\sqrt{1+\left(\frac{\omega}{v\mu_{a0}}\right)^2}-1\right)^{1/2}.$$

Equations (3*a*) and (3*b*) are transcendental equations, and their solution requires the knowledge of 7 parameters: μ_{a0} and μ_{s0}' (known), r, ψ_{DC0} (or ψ_{AC0}), Φ_0, ψ_{DC} (or ψ_{AC}), and Φ (measured). Once D is obtained, μ_a and μ_s' can be derived from the following equations:

using DC and phase:
$$\mu_a = \frac{D}{r^2}\left(\alpha_{DC} - \ln\frac{D}{D_0}\right)^2 \tag{4a}$$

$$\mu_s' = \frac{1}{3D} - \mu_a \tag{4b}$$

using AC and phase:
$$\mu_a = \frac{\omega^2 r^2}{4Dv^2\gamma^2} - \frac{\gamma^2 D}{r^2} \tag{5a}$$

$$\mu_s' = \frac{1}{3D} - \mu_a \tag{5b}$$

3. EXPERIMENTAL METHODS AND RESULTS

We have experimentally verified these theoretical results in the infinite geometry, i.e. with both source and detector deeply immersed in a macroscopically homogeneous, strongly scattering medium. The calibration measurement was performed on an aqueous solution of Liposyn and black India ink. Its

optical parameters (measured with the multi-distance protocol) were $\mu_{a0} = 0.088 \pm 0.003$ cm^{-1} and $\mu_{s0}' = 19.8 \pm 0.4$ cm^{-1}. The light source was an LED emitting at a peak wavelength of 715 nm, and the modulation frequency was selected at 100 MHz. An optical fiber, in direct contact with the LED, was coupled to a reference photomultiplier tube. This reference signal was used to correct for intensity fluctuations of the light source during the experiment and to assign the reference phase value. The instrumental apparatus is the same as that described in Ref. 3. The unknown sample was a scattering aqueous solution of low fat milk. The values of the optical parameters of the sample recovered by applying the pre-calibrated approach were: $\mu_a = 0.0148 \pm 0.0007$ cm^{-1}, $\mu_s' = 11.3 \pm 0.2$ cm^{-1}. To evaluate the accuracy of these results, we independently measured the optical coefficients of the sample with the multi-distance method. We obtained $\mu_a = 0.0125 \pm 0.0002$ cm^{-1}, $\mu_s' = 12.7 \pm 0.1$ cm^{-1}.

The deviations between the results obtained in the two measurement protocols (about 18% for μ_a and 11% for μ_s') are not justified by experimental errors. We attribute these deviations to an inaccurate formal expression for the intercept terms in Eqs. (1*a*), (1*b*) and (1*c*). This inaccuracy does not affect the results of the multi-distance protocol but does affect those of the pre-calibrated protocol. However, the lower accuracy of the pre-calibrated approach is not a major concern for imaging purposes. A systematic error in these values, which affects the readings from all the source-detector pairs to the same extent, will not influence contrast, resolution, and qualitative content of the optical maps. Moreover, since our approach employs equations, which are strictly valid only in the homogeneous case, the recovered values of μ_a and μ_s' in the presence of an inhomogeneity are some sort of average between the values of the inhomogeneity and those of the background. In this sense, our approach is intrinsically incapable of quantitatively determining the optical properties of the inhomogeneity. On the other hand, we observe that the precision of the pre-calibrated protocol is comparable to that of the multi-distance protocol.

We have tested the capability of the pre-calibrated approach to recover the optical properties of an inhomogeneity embedded in a strongly scattering medium, by performing some *in vitro* experiments.

We measured the optical maps relative to two glass spheres (filled with solutions with different optical properties) embedded in a 10 L solution of 50% water and 50% low fat milk. In this experiment, we used the LED emitting at 715 nm as the light source, with intensity modulation at a frequency of 100 MHz, and we collected light with an optical fiber bundle (3 mm in diameter). Both light source and optical fiber were embedded into the medium. The source and the detector, facing each other (separation distance of 4.2 cm), were scanned in tandem in a 5 cm × 4 cm plane, with scanning steps of 2 mm, by using a xyz positioning table. In Fig. 2 we depict the plane containing the centers of the spheres, parallel to the scanning planes containing source and detector.

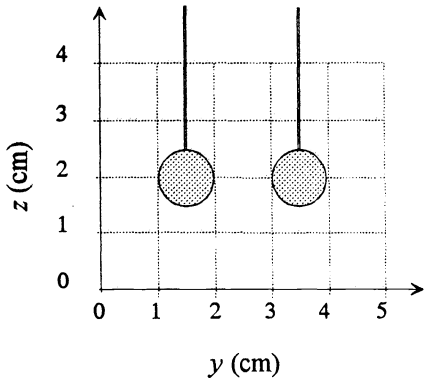

Fig. 2. Plane containing the centers of the two inhomogeneities, corresponding to the scanned area. The two glass spheres have a diameter of 1 cm and the separation between the two centers is 2 cm. The spheres have a long thin neck for filling and positioning purpose. The light source and the detector are scanned simultaneously along the y and z directions in the two parallel planes located at x=-2.1 cm and x=+2.1 cm respectively.

The optical coefficients of the medium (μ_{a0} and μ_{s0}') were recovered using the multi-distance protocol. We found $\mu_{a0} = 0.0131 \pm 0.0005$ cm^{-1} and $\mu_{s0}' = 12.5 \pm 0.1$ cm^{-1}. First, we collected data in the absence of the inhomogeneities to obtain ψ_{DC0} and Φ_0. Then, we introduced the inhomogeneities, filled with one of the following media:

1) the same solution as the surrounding medium ($\mu_a = \mu_{a0}$ and $\mu_s' = \mu_{s0}'$);
2) a solution four times more absorbing than the surrounding medium (by adding black India ink to the 50% water and 50% milk solution), i.e. $\mu_a = 4\ \mu_{a0}$ and $\mu_s' = \mu_{s0}'$;
3) a solution two times more scattering than the surrounding medium (a 100% low fat milk solution), i.e. $\mu_a = \mu_{a0}$ and $\mu_s' = 2\ \mu_{s0}'$.

The acquisition time for each map (made of 500 data points) was about 15 minutes, as a result of the time required for the mechanical raster scan of the light source and fiber optic detector. In Fig. 3, we report the effect of the glass spheres (both filled with solution # 1) in the calculated reduced scattering coefficient μ_s' in two different representations: (a) surface plot, (b) contour graph.

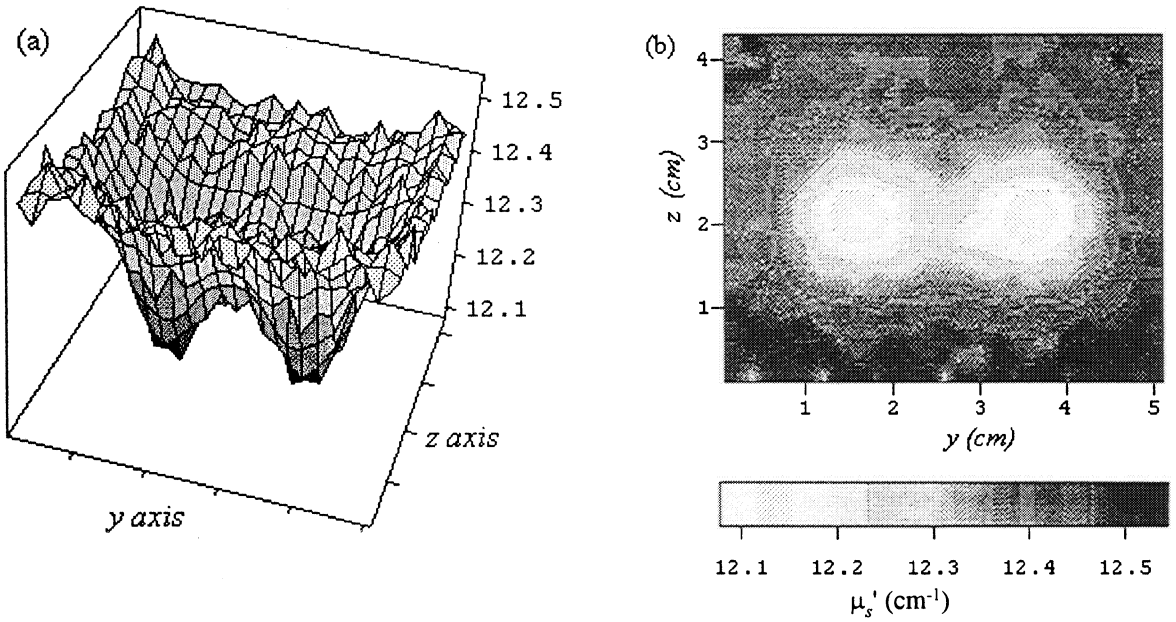

Fig. 3. Effect of the glass in the scattering map. In this experiment, the two glass spheres were filled with the same solution which constitutes the background medium. The scattering map is shown in two different representations: surface plot (panel (a)), and contour graph (panel (b)).

In both representations, one can clearly see the positions of the two spheres, corresponding to the lower scattering areas induced by the glass. For the absorption coefficient, we found a relatively homogeneous map (maximum relative variation of μ_a in the scanned area of 1%). These scattering and absorption maps are used to subtract the effect of the glass in the following maps, where the optical properties of the filling substances are different from the optical properties of the surrounding medium. In this way, only the effect of the filling material is considered.

Figure 4 shows the absorption (panel (a)) and scattering (panel (b)) maps of the two spheres filled with solution # 2 (absorbing). The increase in the absorption coefficient in the area containing the

spheres is in qualitative agreement with their four times higher absorption coefficient with respect to the background. In the scattering map, only a small variation in the reduced scattering coefficient reveals the presence of the two inhomogeneities.

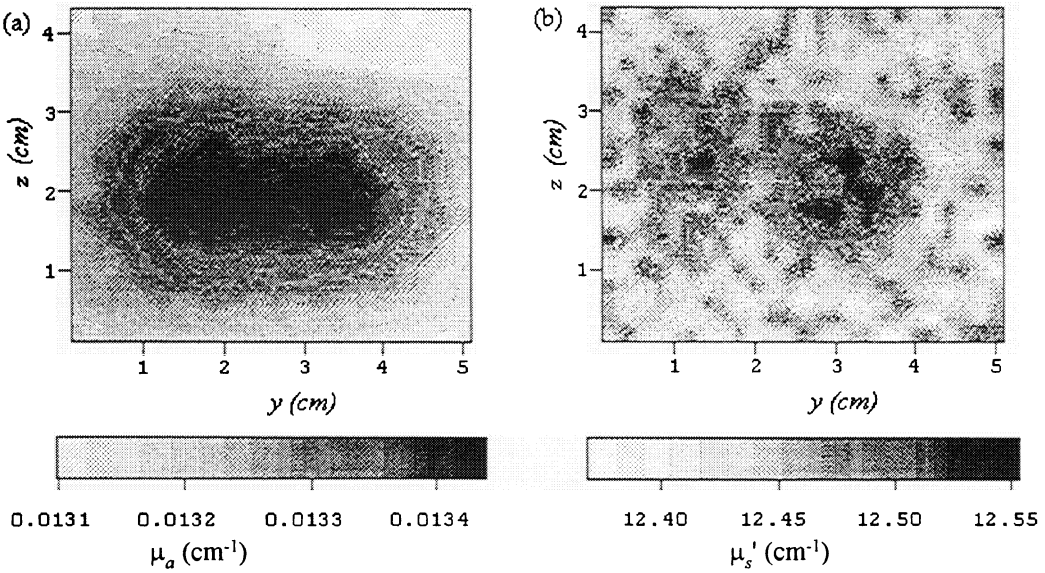

Fig. 4. Absorption (a) and scattering (b) maps of two inhomogeneities more absorbing than the background.

Figure 5 shows the absorption and scattering maps of the two spheres, where the left one is filled with solution # 2 (absorbing) and the right one with solution # 3 (scattering). As expected, the absorbing map (panel (a)) reveals only the absorbing sphere (the one on the left), while the scattering map (panel (b)) reveals only the scattering sphere (the one on the right).

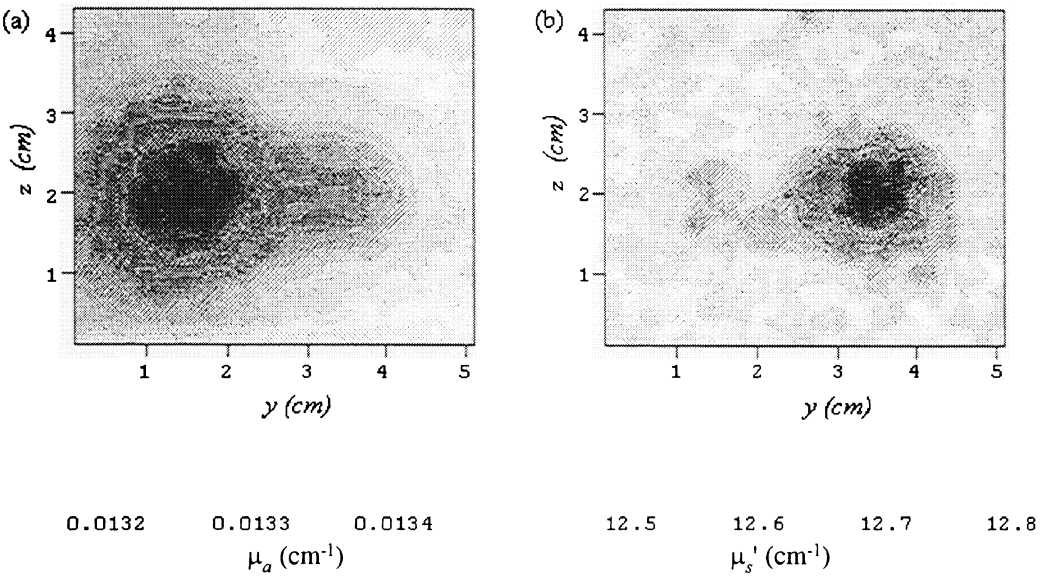

Fig. 5. Absorbing (a) and scattering (b) maps of two inhomogeneities with different optical properties. The left one is more absorbing than the background, the right one is more scattering than the background.

To conclude, we want to show the results obtained using a totally different inhomogeneity: lamb ribs. A slab of lamb ribs with three bones was embedded in the previously described highly scattering medium and scanned using the same light source and fiber optics detector. The scanned area was 8 cm × 4 cm with scanning steps of 2 mm for a total acquisition time of about 25 min. In Fig. 6 we report the scanned area containing the ribs.

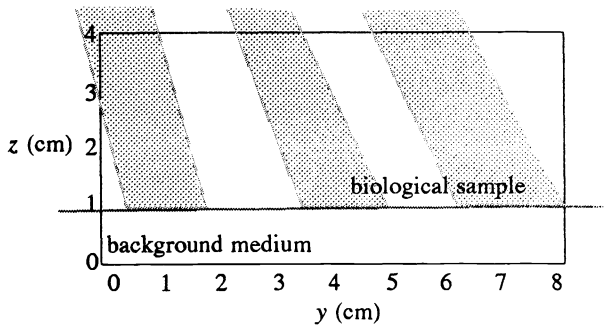

Fig. 6. Scanned area showing the positions of the lamb ribs. The biological sample extends from about $z = 1$ cm to $z = 6$ cm and $y = -3$ cm to $y = 11$ cm. The thickness of the ribs is about 1 cm. The positions of the bones are indicated by the shaded areas.

The resulting optical maps are shown in Fig. 7. The boundary effect at the edge of the slab of the ribs strongly influences the absorption map in the z direction in panel (a). This boundary effect is less evident in the scattering map (panel (b)). The three bones are clearly resolved in the scattering map as a result of the different scattering properties of bones and soft tissue (flesh).

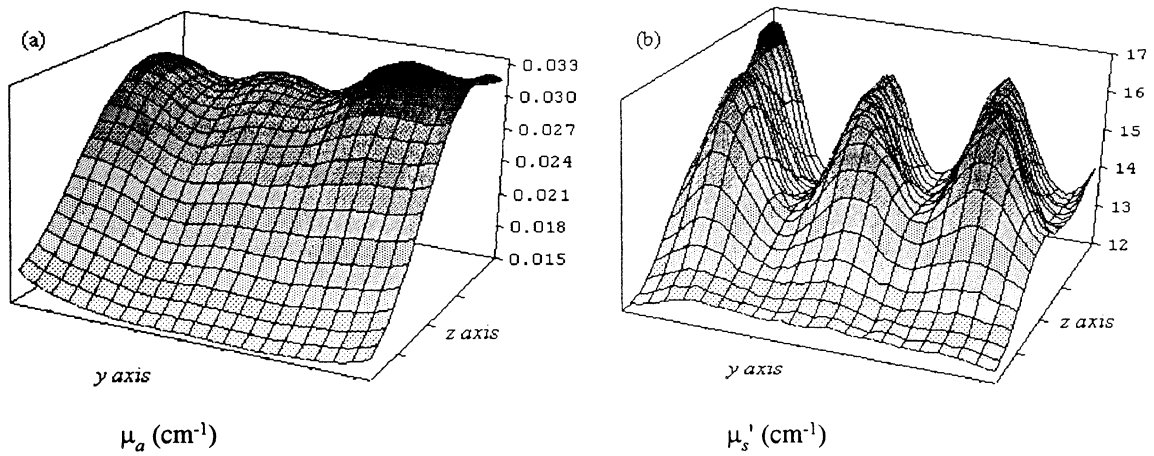

μ_a (cm^{-1}) μ_s' (cm^{-1})

Fig. 7. Absorption (a) and scattering (b) maps of a slab of lamb ribs. The positions of the bones are clearly visible, especially in the scattering map.

6. DISCUSSION AND CONCLUSIONS

The study presented in this paper constitutes a necessary first step in evaluating the effectiveness of a back-projection method for tomographic reconstruction. If a measurement of μ_a and μ_s' in the presence of a macroscopic inhomogeneity can give information on the optical nature (absorbing or scattering) of the inhomogeneity, then a back-projection method should succeed in providing a qualitative optical map

of the medium. Following this approach, 3-D images of defects embedded in turbid media have been obtained.[5] In the cases considered in this paper, we were able to correctly recover the optical nature of the inhomogeneities, by simply using the equations valid for homogeneous media. This approach requires that the inhomogeneities constitute a small perturbation to the homogeneous case. The quantitative determination of μ_a and μ_s', and the effective separation of the effects on the measurable parameters due to absorption and scattering, are results attainable in the homogeneous case. These two results are only approximately reproduced in the presence of defects. Figure 4 shows that absorbing spheres cause a more evident effect in the absorption map than in the scattering map. Still, the scattering map is not totally flat, meaning that the separation between μ_a and μ_s' is not complete. Also, the determination of μ_a is obviously not quantitative, since only a fraction of the photon path-lengths probe the inhomogeneity. However, we believe that even a qualitative optical map, in conjunction with the high speed of the back-projection algorithm, could be of great interest in optical tomography. Our experimental results also show another interesting feature. The scattering image (Fig. 5 (b)) is better resolved than the absorption image (Fig. 5 (a)). This result is related to a narrower scattering weight function with respect to the absorption weight function.[1] Finally, we stress that the high precision of the pre-calibrated measurement protocol enables us to detect changes of a few percent in the measured optical parameters.

A question arises about the limits of the approach presented in this paper. We are currently studying the effectiveness of the qualitative determination of μ_a and μ_s' when:

1. many inhomogeneities are present;
2. the inhomogeneities have optical properties strongly different from those of the background medium;
3. the size and dimensions of the inhomogeneity are arbitrary.

These results, all relative to the infinite space, will have to be generalized to the semi-infinite space, that describe the noninvasive approach in reflection mode. The geometrical distribution of light sources and optical detector in the imaging instrument will be dictated by the results of our preliminary research.

5. ACKNOWLEDGMENTS

This work was performed at the Laboratory for Fluorescence Dynamics at the University of Illinois at Urbana-Champaign (UIUC), which is supported by the National Institutes of Health (NIH), grant RR03155 and by UIUC. This research is also supported by grant CA57032 from the NIH.

6. REFERENCES

1. S. Fantini, M. A. Franceschini, S. A. Walker, J. S. Maier, and E. Gratton, "Photon Path Distributions in Turbid Media: Applications for Imaging" in *Optical Tomography, Photon Migration, and Spectroscopy of Tissue and Model Media: Theory, Human Studies, and Instrumentation*, Proc. SPIE **2389** (1995).
2. J. B. Fishkin and E. Gratton, "Propagation of Photon-Density Waves in Strongly Scattering Media Containing an Absorbing Semi-Infinite Plane Bounded by a Straight Edge," J. Opt. Soc. Am. A **10**, 127-140 (1993).

3. S. Fantini, M. A. Franceschini, J. B. Fishkin, B. Barbieri, and E. Gratton, "Quantitative Determination of the Absorption Spectra of Chromophores in Strongly Scattering Media: a Light-Emitting-Diode Based Technique," Appl. Opt. **33**, 5204-5213 (1994).

4. J. B. Fishkin, P. T. C. So, A. E. Cerussi, S. Fantini, M. A. Franceschini, and E. Gratton, "A Frequency-Domain Method for Measuring Spectral Properties in Multiply Scattering Media: Methemoglobin Absorption Spectrum in a Tissue-Like Phantom," Appl. Opt. (*in press*).

5. S. A. Walker, A. E. Cerussi, and E. Gratton, "Back-Projection Image Reconstruction Using Photon Density Waves in Tissues," in *Optical Tomography, Photon Migration, and Spectroscopy of Tissue and Model Media: Theory, Human Studies, and Instrumentation*, Proc. SPIE **2389** (1995).